

MULTI-SCALE CREEP ANALYSIS OF LONG FIBER-REINFORCED LAMINATES

Yuichi Fukuta*, Tetsuya Matsuda*, Masamichi Kawai*

*Department of Engineering Mechanics and Energy, University of Tsukuba

Keywords: *long fiber-reinforced laminate, creep, multi-scale, homogenization*

Abstract

In this study, multi-scale creep analysis of long fiber-reinforced laminates under in-plane uniaxial load is performed based on a homogenization theory. First, the homogenization theory for nonlinear time-dependent composites is applied to long fiber-reinforced laminates, leading to the macroscopic rate-type constitutive equation of laminates and the evolution equations of microscopic and average stresses in each lamina. The macroscopic constitutive equation is shown to have a stiffness tensor and a stress relaxation function which are evaluated explicitly in terms of the microscopic structure and stacking sequence of laminae. The present theory is then applied to analyzing the in-plane creep behavior of unidirectional carbon fiber/epoxy laminates. It is thus shown that the theory is successful in analyzing the anisotropic creep behavior of unidirectional CFRP laminates.

1 Introduction

Long fiber-reinforced laminates are now important engineering materials. In general, these laminates consist of laminae, each of which is unidirectionally reinforced with long fibers. Macroscopic responses of laminates are therefore usually predicted by attaining the overall responses of monolayers (laminae) and then by averaging them in accordance with the stacking sequence of laminae. Appropriate methods such as the Mori-Tanaka theory [1] and the cell model of Aboudi [2] can be employed for attaining the overall responses of monolayers [3-6]. These models are based on approximate fields of microscopic stress and strain and are fairly successful, but may have errors especially when inelastic deformation occurs in constituents. It is, therefore, worthy developing a theory by which the inelastic behavior of fiber-reinforced laminates can be simulated accurately.

The authors constructed a homogenization theory for nonlinear time-dependent composites with periodic microstructures [7,8]. This theory is based on unit cell problems, in which the so-called Y -periodicity of perturbed displacement is utilized as its boundary condition [9-12]. The theory analyzes not only the macroscopic elastic-viscoplastic behavior of composites but also the microscopic time-dependent distributions of stress and strain in unit cells. Ohno et al. [13] further showed that if the microscopic distributions of stress and strain are symmetric with respect to the center of each unit cell, the field of perturbed velocity satisfies the point symmetry with respect to the cell boundary facet centers: Consequently, semiunit cells can be taken as the domain of analysis to reduce computational efforts. The homogenization theory was thus rebuilt using semiunit cells and applied for computing elastic-viscoplastic behavior of fiber-reinforced unidirectional composites.

The homogenization theory mentioned above does not need any approximation of microscopic stress and strain fields, if the Y -periodicity of microstructures can be assumed. Thus, we expect that the theory accurately predicts the macroscopic time-dependent behavior of fiber-reinforced laminates, if we can establish a framework to apply the theory to such laminates. In addition, we notice that the theory allows us to analyze the microscopic distributions of stress and strain in each lamina. These merits cannot be available if other theories are employed. It is, therefore, of significance to employ the homogenization theory for simulating the time-dependent nonlinear behavior of fiber-reinforced laminates. For this reason, the author has already applied the theory to the elastic-viscoplastic analysis of CFRP laminates [14,15]. The theory, however, has not been applied to analyzing the creep behavior of laminates so far.

In this paper, the in-plane creep behavior of long fiber-reinforced laminates at high temperature

is analyzed based on the homogenization theory for nonlinear time-dependent composites. The macroscopic equation is shown to be characterized by a stiffness tensor and a stress relaxation function which are evaluated in terms of the microscopic structure and stacking sequence of laminae. Using the present theory, the analysis of in-plane creep deformation of unidirectional laminates at high temperature is performed. It is thus shown that the analysis results agree well with the experimental data. Moreover, the off-axis creep behavior with seven kinds of off-axis angles is analyzed, showing the marked in-plane creep anisotropy of the unidirectional laminates.

2 Theory

2.1 Basic Assumptions

Let us consider a laminate in which long fiber-reinforced laminae are stacked symmetrically as shown in Fig. 1. Let us assume that the fibers are arranged unidirectionally and periodically in each lamina, as illustrated in the figure, and also that the fibers deform elastically while the matrix exhibit elasticity and viscoplasticity. Let N and $f^{(\alpha)}$ be the number of laminae and the volume fraction of the α th lamina, respectively. It is convenient to use three kinds of Cartesian coordinates, i.e., X_i ($i=1, 2, 3$) for the laminate, $x_i^{(\alpha)}$ ($i=1, 2, 3$) for the α th lamina, and $y_i^{(\alpha)}$ ($i=1, 2, 3$) for the unit cell in the α th lamina, $Y^{(\alpha)}$, as shown in Fig. 1. The X_2

axis is taken in the stacking direction. The $x_2^{(\alpha)}$ -axis is parallel to the X_2 -axis and thus directed perpendicularly to the lateral surface of the α th lamina. The $x_3^{(\alpha)}$ -axis is taken in the fiber direction of the α th lamina and makes an angle $\theta^{(\alpha)}$ with the X_3 axis. The $y_i^{(\alpha)}$ -axis is parallel to the $x_i^{(\alpha)}$ -axis but is employed solely for the unit cell $Y^{(\alpha)}$.

Let us assume further that the laminate which is infinitely large in the X_1 - and X_3 -directions, is subject to in-plane loading, giving rise to no bending because of the symmetry in stacking. Then, the macroscopic stress in the laminate, Σ_{ij} , and the overall stresses in laminae, $\Sigma_{ij}^{(\alpha)}$, satisfy

$$\Sigma_{ij} = \sum_{\alpha=1}^N f^{(\alpha)} \Sigma_{ij}^{(\alpha)}, \text{ in-plane components, } (1)$$

$$\Sigma_{22} = \Sigma_{21} = \Sigma_{23} = 0, (2)$$

$${}_X \Sigma_{22}^{(\alpha)} = {}_X \Sigma_{21}^{(\alpha)} = {}_X \Sigma_{23}^{(\alpha)} = 0, \alpha = 1, 2, \dots, N, (3)$$

where ${}_X(\)$ stands for the components with respect to the X_i coordinate system. The macroscopic strain in the laminate, E_{ij} , and the overall strains in laminae, $E_{ij}^{(\alpha)}$, can be expressed as

$$E_{11} = {}_X E_{11}^{(\alpha)}, E_{33} = {}_X E_{33}^{(\alpha)}, E_{13} = {}_X E_{13}^{(\alpha)}, \alpha = 1, 2, \dots, N, (4)$$

$$E_{22} = \sum_{\alpha=1}^N f^{(\alpha)} {}_X E_{22}^{(\alpha)}, (5)$$

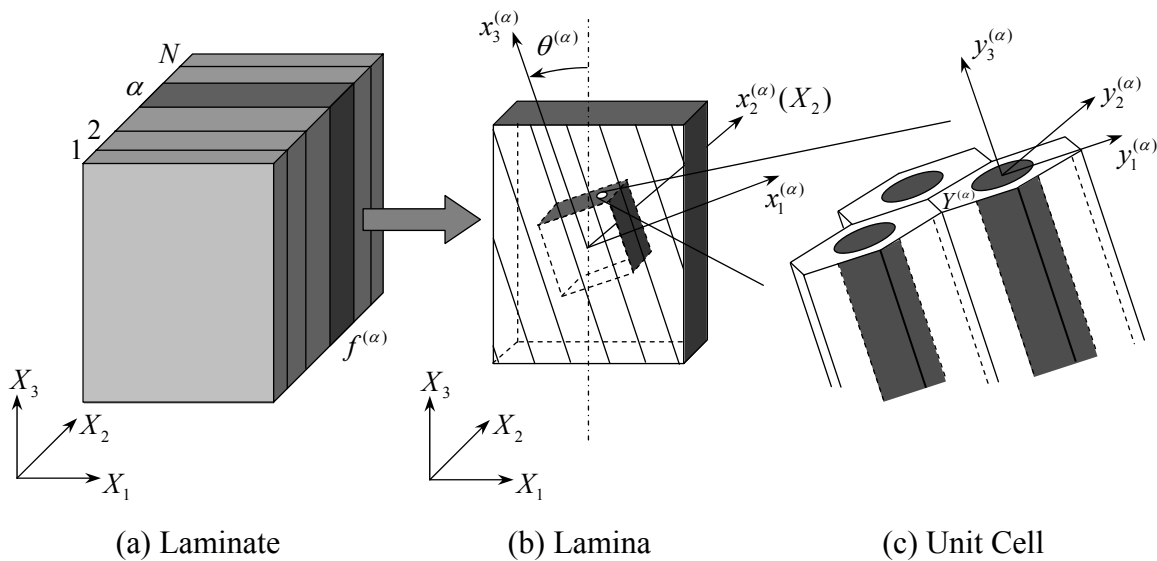


Fig. 1. Structure of a laminate and three kinds of Cartesian coordinates.

$$E_{21} = E_{23} = 0, \quad (6)$$

$${}_x E_{21}^{(\alpha)} = {}_x E_{23}^{(\alpha)} = 0, \quad \alpha = 1, 2, \dots, N. \quad (7)$$

Equations 3 and 7 also hold with respect to the $x_i^{(\alpha)}$ coordinate system:

$${}_x \Sigma_{22}^{(\alpha)} = {}_x \Sigma_{21}^{(\alpha)} = {}_x \Sigma_{23}^{(\alpha)} = 0, \quad \alpha = 1, 2, \dots, N, \quad (8)$$

$${}_x E_{21}^{(\alpha)} = {}_x E_{23}^{(\alpha)} = 0, \quad \alpha = 1, 2, \dots, N. \quad (9)$$

2.2 Homogenization in Laminae

Let us denote the microscopic distributions of stress and strain in the unit cell $Y^{(\alpha)}$ of the α th lamina as $\sigma_{ij}^{(\alpha)}(\mathbf{y}, t)$ and $\varepsilon_{ij}^{(\alpha)}(\mathbf{y}, t)$, where \mathbf{y} and t denote y_i and time, respectively. Then, the overall stress and strain in the α th lamina, ${}_x \Sigma_{ij}^{(\alpha)}$ and ${}_x E_{ij}^{(\alpha)}$, are evaluated by homogenizing $\sigma_{ij}^{(\alpha)}(\mathbf{y}, t)$ and $\varepsilon_{ij}^{(\alpha)}(\mathbf{y}, t)$ using a volume average

$$\langle \# \rangle = \frac{1}{|Y^{(\alpha)}|} \int_{Y^{(\alpha)}} \# \, dY^{(\alpha)}, \quad (10)$$

where $|Y^{(\alpha)}|$ indicates the volume of $Y^{(\alpha)}$. Thus,

$${}_x \Sigma_{ij}^{(\alpha)} = \langle \sigma_{ij}^{(\alpha)} \rangle, \quad (11)$$

$${}_x E_{ij}^{(\alpha)} = \langle \varepsilon_{ij}^{(\alpha)} \rangle. \quad (12)$$

We assume that the microscopic stress $\sigma_{ij}^{(\alpha)}$ and strain $\varepsilon_{ij}^{(\alpha)}$ are related by a constitutive relation

$$\dot{\sigma}_{ij}^{(\alpha)} = c_{ijkl}^{(\alpha)} [\dot{\varepsilon}_{kl}^{(\alpha)} - \beta_{kl}^{(\alpha)}], \quad (13)$$

where $(\dot{})$ denotes the differentiation with respect to t , and $c_{ijkl}^{(\alpha)}$ and $\beta_{kl}^{(\alpha)}$ indicate elastic stiffness and viscoplastic rate satisfying $c_{ijkl}^{(\alpha)} = c_{jikl}^{(\alpha)} = c_{ijlk}^{(\alpha)} = c_{klij}^{(\alpha)}$ and $\beta_{kl}^{(\alpha)} = \beta_{lk}^{(\alpha)}$, respectively. It is noted that $c_{ijkl}^{(\alpha)}$ and $\beta_{kl}^{(\alpha)}$ change from constituent to constituent in each lamina, and that $\beta_{kl}^{(\alpha)}$ vanishes in the fibers.

Then, we can show the following relations which satisfy all fundamental equations such as the equilibrium equation of stress, the relation between displacement and strain and the constitutive relation [7,8]:

$$\dot{\sigma}_{ij}^{(\alpha)}(\mathbf{y}, t) = a_{ijkl}^{(\alpha)}(\mathbf{y}, t) {}_x \dot{\varepsilon}_{kl}^{(\alpha)}(t) - r_{ij}^{(\alpha)}(\mathbf{y}, t), \quad (14)$$

$${}_x \dot{\Sigma}_{ij}^{(\alpha)} = \langle a_{ijkl}^{(\alpha)} \rangle {}_x \dot{\varepsilon}_{kl}^{(\alpha)} - \langle r_{ij}^{(\alpha)} \rangle, \quad (15)$$

where

$$a_{ijkl}^{(\alpha)} = c_{ijpq}^{(\alpha)} (\delta_{pk} \delta_{ql} + \chi_{p,q}^{kl(\alpha)}), \quad (16)$$

$$r_{ij}^{(\alpha)} = c_{ijkl}^{(\alpha)} (\beta_{kl}^{(\alpha)} + \varphi_{k,l}^{(\alpha)}). \quad (17)$$

Here, δ_{ij} denotes Kronecker's delta, $(\)_j$ indicates the differentiation with respect to y_j , and $\chi_i^{kl(\alpha)}$ and $\varphi_i^{(\alpha)}$ are the functions to be determined by solving boundary value problems

$$\int_{Y^{(\alpha)}} c_{ijpq}^{(\alpha)} \chi_{p,q}^{kl(\alpha)} v_{i,j}^{(\alpha)} dY^{(\alpha)} = - \int_{Y^{(\alpha)}} c_{ijkl}^{(\alpha)} v_{i,j}^{(\alpha)} dY^{(\alpha)}, \quad (18)$$

$$\int_{Y^{(\alpha)}} c_{ijpq}^{(\alpha)} \varphi_{p,q}^{(\alpha)} v_{i,j}^{(\alpha)} dY^{(\alpha)} = - \int_{Y^{(\alpha)}} c_{ijkl}^{(\alpha)} \beta_{kl}^{(\alpha)} v_{i,j}^{(\alpha)} dY^{(\alpha)}, \quad (19)$$

where $v_i^{(\alpha)}$ signifies any Y -periodic velocity field defined in $Y^{(\alpha)}$ at t .

2.3 In-Plane Elastic-Viscoplastic Constitutive Equation of Laminates

Solving Eq. 15 for ${}_x \dot{E}_{ij}^{(\alpha)}$ and transforming the resulting equation to a matrix form gives:

$$\{ {}_x \dot{E}^{(\alpha)} \}_{6 \times 1} = [B^{(\alpha)}]_{6 \times 6} \{ {}_x \dot{\Sigma}^{(\alpha)} \}_{6 \times 1} + \{ C^{(\alpha)} \}_{6 \times 1}. \quad (20)$$

Then, Eqs. 8 and 9 allow the above equation to be reduced to

$$\{ {}_x \bar{E}^{(\alpha)} \}_{3 \times 1} = [\bar{B}^{(\alpha)}]_{3 \times 3} \{ {}_x \bar{\Sigma}^{(\alpha)} \}_{3 \times 1} + \{ \bar{C}^{(\alpha)} \}_{3 \times 1}, \quad (21)$$

$${}_x \dot{E}_{22}^{(\alpha)} = B_{21}^{(\alpha)} {}_x \dot{\Sigma}_{11}^{(\alpha)} + B_{23}^{(\alpha)} {}_x \dot{\Sigma}_{33}^{(\alpha)} + B_{26}^{(\alpha)} {}_x \dot{\Sigma}_{31}^{(\alpha)} + C_{22}^{(\alpha)}, \quad (22)$$

where $(\bar{})$ stands for the in-plane parts, i.e.,

$$\{ {}_x \bar{\Sigma}^{(\alpha)} \} = \{ {}_x \dot{\Sigma}_{11}^{(\alpha)} \quad {}_x \dot{\Sigma}_{33}^{(\alpha)} \quad {}_x \dot{\Sigma}_{31}^{(\alpha)} \}^T, \quad (23)$$

$$\{ {}_x \bar{E}^{(\alpha)} \} = \{ {}_x \dot{E}_{11}^{(\alpha)} \quad {}_x \dot{E}_{33}^{(\alpha)} \quad 2 {}_x \dot{E}_{31}^{(\alpha)} \}^T, \quad (24)$$

and so on. Here $(\)^T$ denotes the transpose.

Now, let us introduce further the in-plane vectors of ${}_x \dot{\Sigma}_{ij}^{(\alpha)}$ and ${}_x \dot{E}_{ij}^{(\alpha)}$, i.e.,

$$\{ {}_x \bar{\Sigma}^{(\alpha)} \} = \{ {}_x \dot{\Sigma}_{11}^{(\alpha)} \quad {}_x \dot{\Sigma}_{33}^{(\alpha)} \quad {}_x \dot{\Sigma}_{31}^{(\alpha)} \}^T, \quad (25)$$

$$\{ {}_x \bar{E}^{(\alpha)} \} = \{ {}_x \dot{E}_{11}^{(\alpha)} \quad {}_x \dot{E}_{33}^{(\alpha)} \quad 2 {}_x \dot{E}_{31}^{(\alpha)} \}^T. \quad (26)$$

Then, since the $x_1^{(\alpha)}$ - and $x_3^{(\alpha)}$ -axes make respectively an angle $\theta^{(\alpha)}$ with the X_1 - and X_3 -axes (see Fig. 1), we have

$$\left\{ {}_x \bar{\Sigma}^{(\alpha)} \right\} = [P^{(\alpha)}] \left\{ {}_x \bar{\Sigma}^{(\alpha)} \right\}, \quad (27)$$

$$\left\{ {}_x \bar{E}^{(\alpha)} \right\} = [Q^{(\alpha)}] \left\{ {}_x \bar{E}^{(\alpha)} \right\}, \quad (28)$$

where

$$[P^{(\alpha)}] = \begin{bmatrix} [c^{(\alpha)}]^2 & [s^{(\alpha)}]^2 & 2c^{(\alpha)}s^{(\alpha)} \\ [s^{(\alpha)}]^2 & [c^{(\alpha)}]^2 & -2c^{(\alpha)}s^{(\alpha)} \\ -c^{(\alpha)}s^{(\alpha)} & c^{(\alpha)}s^{(\alpha)} & [c^{(\alpha)}]^2 - [s^{(\alpha)}]^2 \end{bmatrix}, \quad (29)$$

$$[Q^{(\alpha)}] = \begin{bmatrix} [c^{(\alpha)}]^2 & [s^{(\alpha)}]^2 & c^{(\alpha)}s^{(\alpha)} \\ [s^{(\alpha)}]^2 & [c^{(\alpha)}]^2 & -c^{(\alpha)}s^{(\alpha)} \\ -2c^{(\alpha)}s^{(\alpha)} & 2c^{(\alpha)}s^{(\alpha)} & [c^{(\alpha)}]^2 - [s^{(\alpha)}]^2 \end{bmatrix}. \quad (30)$$

$$c^{(\alpha)} \equiv \cos \theta^{(\alpha)}, \quad s^{(\alpha)} \equiv \sin \theta^{(\alpha)} \quad (31)$$

Substituting Eqs. 27 and 28 into (21) yields

$$\left\{ {}_x \bar{\Sigma}^{(\alpha)} \right\} = [P^{(\alpha)}]^{-1} [\bar{B}^{(\alpha)}]^{-1} [Q^{(\alpha)}] \left\{ {}_x \bar{E}^{(\alpha)} \right\} - [P^{(\alpha)}]^{-1} [\bar{B}^{(\alpha)}]^{-1} \left\{ \bar{C}^{(\alpha)} \right\}. \quad (32)$$

Finally, substituting Eqs. 32 and 4 into Eq. 1, we obtain a macroscopic in-plane constitutive equation

$$\left\{ \bar{\Sigma} \right\} = [\bar{A}] \left\{ \bar{E} \right\} - \left\{ \bar{R} \right\}, \quad (33)$$

where

$$[\bar{A}] = \sum_{\alpha=1}^N f^{(\alpha)} [P^{(\alpha)}]^{-1} [\bar{B}^{(\alpha)}]^{-1} [Q^{(\alpha)}], \quad (34)$$

$$\left\{ \bar{R} \right\} = \sum_{\alpha=1}^N f^{(\alpha)} [P^{(\alpha)}]^{-1} [\bar{B}^{(\alpha)}]^{-1} \left\{ \bar{C}^{(\alpha)} \right\}. \quad (35)$$

It is noted that $[\bar{A}]$ and $\left\{ \bar{R} \right\}$ in the macroscopic constitutive relation (33) depend on $f^{(\alpha)}$, $\theta^{(\alpha)}$ and $[\bar{B}^{(\alpha)}]$, which are evaluated in terms of the stacking sequence and microscopic structure of laminae.

2.4 Computation

Let us suppose that the history of either Σ_{ij} or E_{ij} , or a combination of them, is prescribed, and that the values of ${}_x \Sigma_{ij}^{(\alpha)}$ and the distributions of $\sigma_{ij}^{(\alpha)}$ and

internal variables in $Y^{(\alpha)}$ are known in all laminae at a current time t . Then, the increments in an interval from t to $t + \Delta t$ are computed as follows:

- (1) The boundary value problems Eqs. 18 and 19 are solved using FEM to determine $\chi_i^{kl(\alpha)}(\mathbf{y}, t)$ and $\varphi_i^{(\alpha)}(\mathbf{y}, t)$, where $\alpha = 1, 2, \dots, N$.
- (2) Compute $\langle a_{ijkl}^{(\alpha)} \rangle$ and $\langle r_{ij}^{(\alpha)} \rangle$, leading to $[\bar{B}^{(\alpha)}]$ and $\left\{ \bar{C}^{(\alpha)} \right\}$ in Eq. 21 and further to $[\bar{A}]$ and $\left\{ \bar{R} \right\}$ using Eqs. 34 and 35.
- (3) Determine the unknown components of $\left\{ \bar{\Sigma} \right\}$ and $\left\{ \bar{E} \right\}$ using Eq. 33 with the prescribed components of $\left\{ \bar{\Sigma} \right\}$ and $\left\{ \bar{E} \right\}$.
- (4) Using Eqs. 27, 28 and 32 with 4, determine $\left\{ {}_x \bar{\Sigma}^{(\alpha)} \right\}$ and $\left\{ {}_x \bar{E}^{(\alpha)} \right\}$.
- (5) From Eqs. 22 and 14, evaluate ${}_x \dot{E}_{22}^{(\alpha)}$ and $\left\{ \dot{\sigma}^{(\alpha)} \right\}$.
- (6) Calculate the increments in the interval from t to $t + \Delta t$ as $\Delta \Sigma_{ij} = \dot{\Sigma}_{ij} \Delta t$, $\Delta \sigma_{ij}^{(\alpha)} = \dot{\sigma}_{ij}^{(\alpha)} \Delta t$, etc., and add the increments to the current values.

3 Analysis

3.1 Long Fiber-Reinforced Laminate and Loading conditions

In the present analysis, we considered a unidirectional carbon fiber/epoxy laminate (T800H/#3631, TORAY) as the simplest case of the long fiber-reinforced laminates. For this laminate, Two kinds of creep analyses were performed. First, the 45° off-axis creep behavior of the laminate at 100°C is analyzed at three kinds of creep stress levels. Then, the creep deformations of the laminate at a constant creep stress (70MPa) and high temperature (100°C) are simulated with seven kinds of off-axis angles, i.e., $\psi = 0^\circ, 10^\circ, 30^\circ, 45^\circ, 60^\circ, 75^\circ, 90^\circ$. The creep analysis of multi-directional laminates will be dealt with in our future works.

3.2 Fiber Arrangement

The arrangement of carbon fibers, which was unidirectional in the $x_3^{(\alpha)}$ direction, was modeled to be hexagonally periodic on the $x_1^{(\alpha)} - x_2^{(\alpha)}$ plane in each lamina, as illustrated in Figs. 1 and 2(a). This is an idealization of the random distribution of fibers on that plane. The idealization can be justified as follows: The hexagonal periodicity of carbon fiber arrangement gives rise to the transverse quasi-isotropy not only in elasticity but also in elastoviscoplasticity [7,8]. Such isotropy matches with the transverse isotropy brought about by the random distribution of fibers on the $x_1^{(\alpha)} - x_2^{(\alpha)}$ plane.

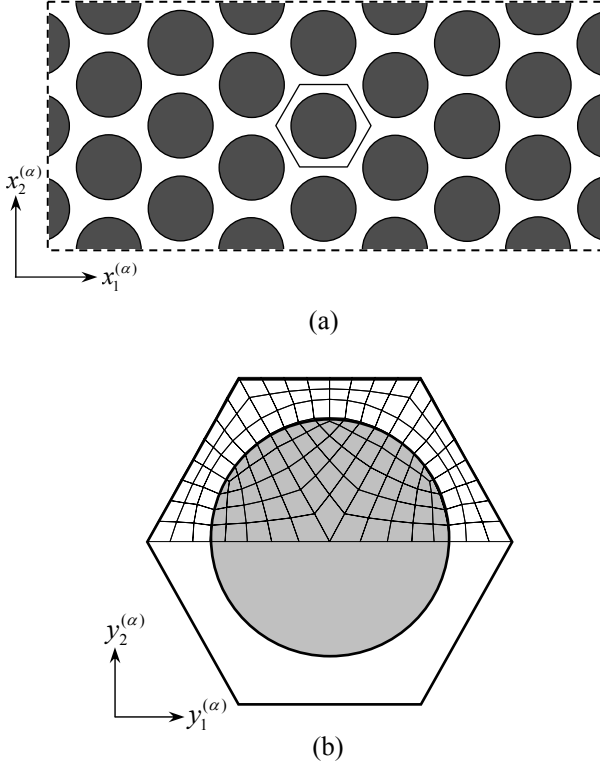


Fig. 2. Microstructure of laminae; (a) hexagonal arrangement of fibers, and (b) unit cell $Y^{(\alpha)}$ and finite element mesh.

The hexagonal periodicity is therefore an appropriate assumption as far as the overall response of each lamina is concerned.

According to the above assumption, the unit cell $Y^{(\alpha)}$ was chosen to be hexagonal for all laminae, as shown in Fig. 2(b); V_f was taken to be 51.7%. Here it is noted that $Y^{(\alpha)}$ was taken to be 2D rather than 3D since each lamina was assumed to have no microscopic variation in the fiber direction [8,16]. Since the hexagonal unit cell has the point symmetry with respect to the cell center, it is sufficient to consider half of the unit cell as the domain of analysis for solving the boundary value problems Eqs. 18 and 19 [13-15]. Hence, the upper half of the unit cell was considered and was divided into finite elements using four-node isoparametric elements, as shown in Fig. 2(b).

3.3 Microscopic Constitutive Equations

The carbon fibers were regarded as a transversely isotropic elastic material. Consequently, the fibers were supposed to have five independent elastic constants, i.e., two Young's moduli E_{f1} and E_{f3} , two Poisson's ratios ν_{f12} and ν_{f31} , and one

shear rigidity G_{f31} , where the subscripts 1, 2 and 3 signify the $y_1^{(\alpha)}$, $y_2^{(\alpha)}$ and $y_3^{(\alpha)}$ directions, respectively. Table 1 shows the five constants of fibers employed in the present work; E_{f3} was provided by the manufacturer, while other constants were obtained by referring to Kriz and Stinchcomb [17].

The epoxy matrix, on the other hand, was regarded as an elastic-viscoplastic material characterized as [14,15]

$$\dot{\epsilon}_{ij} = \frac{1+\nu_m}{E_m} \dot{\sigma}_{ij} - \frac{\nu_m}{E_m} \dot{\sigma}_{kk} \delta_{ij} + \frac{3}{2} \dot{\epsilon}_0^p \left[\frac{\sigma_e}{g(\bar{\epsilon}^p)} \right]^n \frac{s_{ij}}{\sigma_e}, \quad (36)$$

where E_m , ν_m and n are material constants, $g(\bar{\epsilon}^p)$ is a material function depending on accumulated viscoplastic strain $\bar{\epsilon}^p = \int [(2/3)\beta_{ij}^{(\alpha)}\beta_{ij}^{(\alpha)}]^{1/2} dt$, $\dot{\epsilon}_0^p$ is a reference strain rate, s_{ij} indicates the deviatoric part of σ_{ij} , and $\sigma_e = [(3/2)s_{ij}s_{ij}]^{1/2}$. The material constants and material function in Eq. 36 were determined by simulating the 45° off-axis tensile tests of the unidirectional laminate at $\dot{E}_{33}=1.0$ and 0.01 mm/min. This was because the effect of matrix viscoplasticity was expected to be significant in such off-axis tests. Table 1 lists the material parameters determined.

3.4 Results of Analysis

First, Fig. 3 shows the high temperature (100°C) creep curves of the unidirectional laminate with the 45° off-axis angle at three kinds of stress levels, i.e. 35, 51 and 68MPa, respectively. In the figure, the solid lines indicate the analysis results obtained using the present theory, whereas the markers stand for the experimental data [18]. As seen from the experimental data, the creep strain becomes larger as the creep stress level increases, showing the clear stress dependence of the in-plane creep behavior. Such creep behavior of the unidirectional CFRP laminate is successfully predicted by the present theory.

Table 1. Material constants.

Carbon fiber	$E_{f1} = 1.58 \times 10^4$	$\nu_{f12} = 0.49$
	$E_{f3} = 2.94 \times 10^5$	$\nu_{f31} = 0.28$
	$G_{f31} = 1.97 \times 10^4$	
Epoxy	$E_m = 3.6 \times 10^3$	$\nu_m = 0.35$
	$\dot{\epsilon}_0^p = 1.67 \times 10^{-4}$	$n = 35$
	$g(\bar{\epsilon}^p) = 115.4(\bar{\epsilon}^p)^{0.185} + 10$	

MPa (stress), mm/mm (strain), s (time).

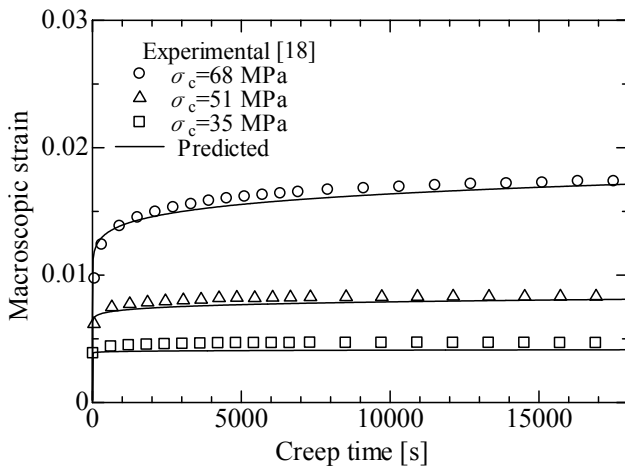


Fig. 3. Macroscopic creep behavior of unidirectional CFRP laminate at three kinds of creep stresses (100°C, $\psi = 45^\circ$).

Next, the high temperature (100°C) creep behavior of the unidirectional laminate with seven kinds of off-axis angles at a constant stress is shown in Fig. 4. The off-axis angles are $\psi = 0^\circ, 10^\circ, 30^\circ, 45^\circ, 60^\circ, 75^\circ, 90^\circ$, and the constant stress is 70MPa. From this figure, we can find that the creep strain hardly occurs at $\psi = 0^\circ$ and 10° . By contrast, the creep strain suddenly increases at $\psi = 30^\circ$, and can be clearly observed. The creep strain increases as the off-axis angle increases, and reaches the maximum at $\psi = 45^\circ$. After that, the creep strain decreases as the off-axis angle increases. These results indicate the marked in-plane creep anisotropy of the unidirectional CFRP laminate.

4 Conclusions

In this study, the homogenization theory for nonlinear time-dependent composites developed by the present authors was employed for predicting the in-plane high temperature creep behavior of long fiber-reinforced laminates. For the present analysis, we derived a macroscopic rate-type constitutive equation of laminates as well as evolution equations of microscopic and average stresses in each lamina based on the homogenization theory. The macroscopic constitutive equation was shown to have a stiffness tensor and a stress relaxation function to be evaluated in terms of the microscopic structure and stacking sequence of laminae. Using the present theory, the in-plane creep analysis of the unidirectional CFRP laminate at high temperature was performed. It was thus shown that the present theory predicted very accurately the macroscopic

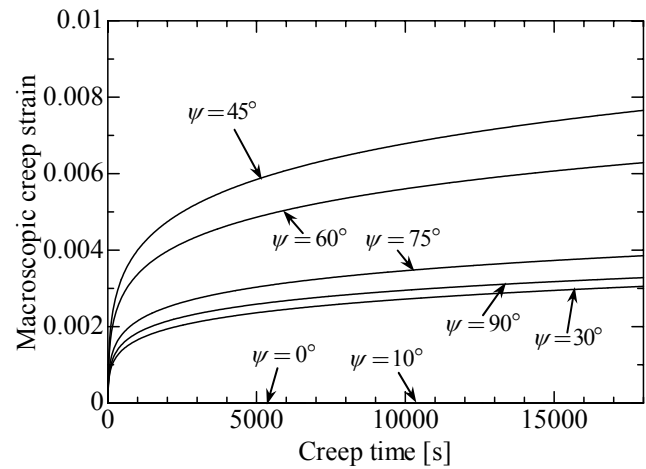


Fig. 4. Macroscopic creep curves for unidirectional CFRP laminate at constant creep stress with various off-axis angles (100°C).

creep behavior of the laminate. It is also shown that the laminate had marked in-plane anisotropy with respect to the creep behavior. The creep analysis of multi-directional laminates should be performed in our future works.

Acknowledgement

The support in part by the Ministry of Education, Culture, Sports, Science and Technology, Japan under a Grant-in-Aid for Young Scientists (B) (No. 18760075) is acknowledged.

References

- [1] Mori T. and Tanaka K. "Average stress in matrix and average elastic energy of materials with misfitting inclusions". *Acta Metall.*, Vol. 21, pp 571-574, 1973.
- [2] Aboudi J. "*Mechanics of composite materials*". Elsevier Science Publishers, 1991.
- [3] Pindera M. J. and Lin M. W. "Micromechanical analysis of the elastoplastic response of metal matrix composites". *ASME J. Press. Vessel Technol.*, Vol. 111, pp 183-190, 1989.
- [4] Tszeng T. C. "Micromechanics characterization of unidirectional composites during multiaxial plastic deformation". *J. Compos. Mater.*, Vol. 28, pp 800-820, 1994.
- [5] Kawai M., Masuko Y., Kawase Y. and Negishi R. "Micromechanical analysis of the off-axis rate-dependent inelastic behavior of unidirectional AS4/PEEK at high temperature". *Int. J. Mech. Sci.*, Vol. 43, pp 2069-2090, 2001.
- [6] Tohgo K., Kawahara K. and Sugiyama Y. "Off-axis tensile properties of CFRP laminates and non-linear

- lamination theory based on micromechanics approach". *Trans. Jpn. Soc. Mech. Eng., Ser. A*, Vol. 67, pp 1493-1500, 2001, (in Japanese).
- [7] Wu X. and Ohno N. "A homogenization theory for time-dependent nonlinear composites with periodic internal structures". *Int. J. Solids Struct.*, Vol. 36, pp 4991-5012, 1999.
- [8] Ohno N., Wu X. and Matsuda T. "Homogenized properties of elastic-viscoplastic composites with periodic internal structures". *Int. J. Mech. Sci.*, Vol. 42, pp 1519-1536, 2000.
- [9] Bensoussan A., Lions J.-L. and Papanicolaou G. "Asymptotic analysis for periodic structures". North-Holland Publishing Company, 1978.
- [10] Sanchez-Palencia E. "Non-homogeneous media and vibration theory. Lecture notes in physics 127". Springer-Verlag, 1980.
- [11] Bakhvalov N. and Panasenko G. "Homogenisation: averaging processes in periodic media". Kluwer Academic Publishers, 1984.
- [12] Guedes J. M. and Kikuchi N. "Preprocessing and postprocessing for materials based on the homogenization method with adaptive finite element methods". *Comput. Methods Appl. Mech. Eng.*, Vol. 83, pp 143-198, 1990.
- [13] Ohno N., Matsuda T. and Wu X. "A homogenization theory for elastic-viscoplastic composites with point symmetry of internal distributions". *Int. J. Solids Struct.*, Vol. 38, pp 2867-2878, 2001.
- [14] Matsuda T., Ohno N., Tanaka H. and Shimizu T. "Homogenized in-plane elastic-viscoplastic behavior of long fiber-reinforced laminates". *JSME Int. J., Ser. A*, Vol. 45, pp 538-544, 2002.
- [15] Matsuda T., Ohno N., Tanaka H. and Shimizu T. "Effects of fiber distribution on elastic-viscoplastic behavior of long fiber-reinforced laminates". *Int. J. Mech. Sci.*, Vol. 45, pp 1583-1598, 2003.
- [16] Noguchi H. and Shimizu E. "Study on fracture mode transition of unidirectional CFRP by using homogenization method (1st Report, Formulation)". *Trans. Jpn. Soc. Mech. Eng., Ser. A*, Vol. 65, pp 225-231, 1999, (in Japanese).
- [17] Kriz R. D. and Stinchcomb W. W. "Elastic moduli of transversely isotropic graphite fibers and their composites". *Exper. Mech.*, Vol. 19, pp 41-49, 1979.
- [18] Kawai M. and Masuko Y. "Creep behavior of unidirectional and angle-ply T800H/3631 laminates at high temperature and simulations using a phenomenological viscoplasticity model". *Compos. Sci. Technol.*, Vol. 64, pp 2373-2384, 2004.